

RSC Advances



This is an *Accepted Manuscript*, which has been through the Royal Society of Chemistry peer review process and has been accepted for publication.

Accepted Manuscripts are published online shortly after acceptance, before technical editing, formatting and proof reading. Using this free service, authors can make their results available to the community, in citable form, before we publish the edited article. This *Accepted Manuscript* will be replaced by the edited, formatted and paginated article as soon as this is available.

You can find more information about *Accepted Manuscripts* in the [Information for Authors](#).

Please note that technical editing may introduce minor changes to the text and/or graphics, which may alter content. The journal's standard [Terms & Conditions](#) and the [Ethical guidelines](#) still apply. In no event shall the Royal Society of Chemistry be held responsible for any errors or omissions in this *Accepted Manuscript* or any consequences arising from the use of any information it contains.

Novel nanocellular poly(aryl ether ketone) foam fabricated by controlling the crosslinking degree

Shisheng Zhu, Zheng Chen, Bing Han, Guibin Wang, Zhenhua Jiang, Shuling Zhang*

Alan G. MacDiarmid Institute, College of Chemistry, Jilin University,

Changchun 130012, People's Republic of China

*Correspondence author: Tel/Fax: (+86) 0431-85168868

E-mail: zsl@jlu.edu.cn**Abstract:**

Films of poly(aryl ether ketone) containing naphthalene pendants on the side chains (NA-PAEK) with different crosslinking degrees were prepared by thermal crosslinking and foamed using a two-stage batch foaming process. The effects of the crosslinking degree on the sorption of CO₂ and foam morphology were investigated. The nucleation rate and foam morphology of the highly elastic polymer was found to depend on the stored elastic energy (SE). Therefore, SE could not be neglected in our system. In addition, the effects of processing parameters such as soaking pressure, soaking time, transferring time, foaming temperature, and foaming time on the foam morphology were investigated. By controlling the crosslinking degree and optimizing the processing parameters, nanocellular poly(aryl ether ketone) foam with a cell size of 86 nm (± 11 nm) was successfully fabricated.

1. Introduction

Cellular plastics are polymeric nanoporous materials with average cell sizes below 1 μm . These materials have attracted great interest in recent years, since they can be used in a variety of applications as templates, low- k materials, sensors, tissue engineering scaffolds, filtration membranes, catalysts, and thermal insulation materials.¹⁻⁴ Compared to traditional materials used in these applications, cellular plastics are more lightweight. Supercritical foaming, which usually involves a foaming agent (typically a gas under supercritical conditions) dissolved in the polymer, is the most attractive method for producing these materials. The foaming agent used in the supercritical foaming process induces phase separation upon heating or pressure quenching. The phase separation is followed by nucleation and cell growth, which occurs until the temperature of the heterogeneous solution drops below the glass transition temperature (T_g) of the plasticised polymer and the pore cells become immobilized within the vitrified polymer matrix.⁵ Supercritical carbon oxide (scCO₂), which is a versatile compressible solvent, has received attention as a physical blowing agent that could be used in polymer foaming, since it is environmentally benign, naturally abundant, and relatively inexpensive.⁶

The simplest method for producing nanocellular materials is to adjust the foam morphology by systematically changing the saturation pressure, saturation time, transferring time, foaming temperature, or depressurization rate. However, decreasing the cell size using this method leads to large increases in the surface energy, which makes the process challenging. Miller *et al.* produced nanocellular polyetherimide (PEI) foam with cell size between 30 and 120 nm by saturating PEI specimens at a pressure of 5 MPa for 300 h, and foaming in the temperature range of 110-145 °C.⁷ However, the long saturation time required renders this method inconvenient. Alternately, heterogeneous nucleating agents can be added to produce nanocellular materials. Costeux *et al.* investigated the foaming behaviour of silica particles and POSS-filled polymethyl methacrylate and styrene acrylonitrile copolymers.⁸ They found that adding less than 0.5 wt. % of a nanoscale additive allowed the production of nanofoams with average cell size of 100 nm, relative density of 0.15 (85% porosity), and cell density exceeding 10^{16} cells/cm³. However, for the successful use of this method, excellent dispersion and exfoliation of the additive are necessary, which is not easy to achieve. Selective swelling of block copolymers using supercritical fluids is another effective method for producing nanocellular materials. By making the dispersed phase more CO₂-philic compared to the surrounding polymer matrix, Yokoyama *et al.* successfully produced nanocellular polystyrene-block-poly(perfluorooctylethyl methacrylate) (PSPFMA) foam.⁹ However, this foaming method is strongly dependent on the properties of the CO₂-philic blocks in the block copolymer, which often limits the choice of blocks to siloxanes and fluoro compounds. This restricts further application of this method.

In this work, a new method for restricting the cell size of nanocellular foams has been proposed. Poly(aryl ether ketone) (PAEK) with naphthalene pendants on the side chains was chosen as the matrix polymer to obtain nanocellular foam under high-temperature conditions.^{10,11} By crosslinking at different temperatures, PAEKs with different crosslinking degrees and gel contents were prepared. Crosslinking is an ideal method for increasing the elasticity of nanocellular foams and changing the foam morphology. The effect of crosslinking degree on CO₂ sorption and the foam morphology was investigated.

2. Experimental

2.1 Materials

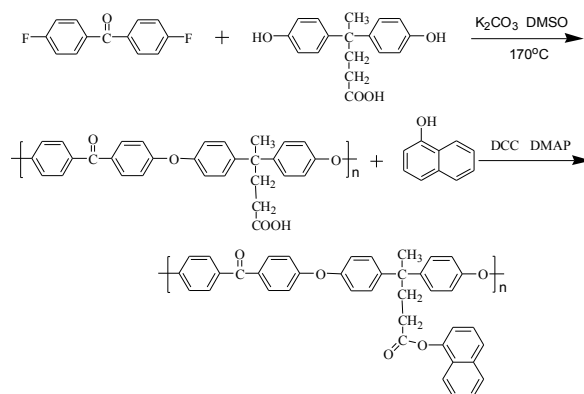
4,4'-Difluoro benzophenone (99%, Yanji Chemical Plant) was used after recrystallization. 4,4'-Bis(4-hydroxyphenyl)pentanoic acid (98%, TCI Chemicals), dicyclohexylcarbodiimide (99%, TCI Chemicals), 4-dimethylaminopyridine (99%, TCI Chemicals), dimethyl sulfoxide (99%, Beijing Chemical Reagent), 1-naphthol (99%, Tianjin Chemical Reagent), and toluene (99%, Beijing Chemical Reagent) were used

as-received. Tetrahydrofuran (Beijing Chemical Reagent) was used after drying and distillation. CO₂ gas with purity greater than 99.99% was obtained from Beijing Analytical Gas Factory, China. The other chemicals used in the experiments were obtained from Beijing Chemical Reagent or Tianjin Chemical Reagent, and used without further purification, unless stated otherwise.

2.2 Sample preparation

2.2.1 Synthesis of PAEK with naphthalene pendants on the side chains (NA-PAEK)

NA-PAEK was synthesized according to the method described in a previous report from our group.¹² The synthesis route and the details of procedure are shown in **Scheme 1** and supporting information, respectively.



Scheme 1 Synthesis route for NA-PAEK

2.2.2 Preparation of NA-PAEK films

NA-PAEK solution was prepared by dissolving NA-PAEK (1 g) in dimethylacetamide (DMAC; 10 mL). The solution was then cast on glass plates to prepare thin NA-PAEK films. The casted films were dried successively in a vacuum oven at 60, 80, 100, and 120 °C for 12, 12, 8, and 4 h, respectively and then removed from the glass plates using a small amount of water. Finally, the films were thermally crosslinked at temperatures of 170, 200, and 250 °C for 2 h under ambient conditions.

2.2.3 Fabrication of NA-PAEK foam

The NA-PAEK foam was prepared using a two-stage batch foaming process. The thermally crosslinked NA-PAEK film was first saturated with CO₂ in a high-pressure vessel at room temperature. The pressure was then suddenly released and the samples were removed from the vessel. The samples were then foamed in an oil bath at a certain foaming temperature for a predetermined length of time, following which the samples were quenched in cold water and washed in ethanol for 1 h. All the foamed samples were dried in a vacuum oven at 60 °C for 24 h prior to measurements.

2.3 Characterization

2.3.1 Measurement of gel content

The gel contents of the thermally crosslinked NA-PAEK films were measured and the crosslinking degree of thermally crosslinked NA-PAEK films was determined using the data. The sample was continuously extracted with THF under reflux for 48 h, then dried in a vacuum oven successively at 80 and 200 °C for 24 and 2 h, respectively. The gel content was expressed by the change in the weight of the NA-PAEK films, and the detailed testing procedure was shown in **Fig.S14**.

2.3.2 Dynamic mechanical analysis

Dynamic mechanical analysis (DMA) was carried out with a TA Instruments DMA Q800 in the tensile mode. All the measurements were performed in the linear with the strain of 0.03%. Storage modulus and $\tan\delta$ of each sample were recorded at a frequency of 1 Hz and a heating rate of 5 °C/min.

2.3.3 Thermal gravimetric analysis

Thermal gravimetric analysis (TGA) was carried out under N₂ atmosphere at a heating rate of 10 °C/min. Samples of 3-5 mg were contained within open platinum pans of a PerkinElmer TGA-7 instrument.

2.3.4 Examination of CO₂ sorption

The gravimetric method, which was reported previously by our group, was applied to study the amounts of CO₂ absorbed and desorbed.¹³ After saturating the sample with CO₂ at a given pressure and temperature, the sample was quickly removed from the high-pressure vessel and placed on the pan of an electronic digital balance (Mettler AS265S). Using a computerized data acquisition system, the weights of the samples during desorption were recorded at short intervals after venting the vessel. The amount of CO₂ absorbed (q) is given by Eq. 1.

$$q = (m_d - m_0)/m_0 \quad (1)$$

where m_0 is the initial weight of the film and m_d is the weight recorded during desorption.

Fickian diffusion was assumed, in order to eliminate the effect of fluid escape during the transfer of the samples from the pressure vessel to the balance, which was given by the following equation.¹⁴

$$\frac{m_d}{m_{t=0}} = \frac{4}{l} \sqrt{\frac{D_d t_d}{\pi}} \quad (2)$$

Where m_d is the weight of sample recorded during desorption, $m_{t=0}$ is the weight when polymer/gas system reach equilibrium, l is the thickness of the sample, D_d is the diffusion coefficient of carbon dioxide, t_d is the recording time.

According to the above equation, if we plot the mass uptake of carbon dioxide with the square root of time, a straight line should be obtained. However, a curve was acquired instead of a straight line because of the swelling

effect. To estimate the CO₂ uptake at t=0, a simple mathematic method was used, the square root of CO₂ concentration was plotted as a function of the logarithm of time, and then a straight line was got and the intercept of the plot allowed us to determine the amount of CO₂ absorbed at zero time.

2.3.5 Examination of the foam morphology

The morphologies of the foam samples were analysed using a SSX-550 SHIMADZU scanning electron microscope (SEM). The samples were freeze-fractured in liquid nitrogen and sputter-coated with gold at an argon pressure of 0.1 Torr for 2 min at a current of 20 mA.

The volume expansion ratio, average cell size and cell density is determined according to the method described by Kumer and Weller.¹⁵

The volume expansion ratio (Φ) is given by the following equation.

$$\Phi = \frac{\rho_p}{\rho_f} \quad (3)$$

Where ρ_p is the density of sample before foaming, whereas ρ_f is the density of the sample after foaming.

The average cell size and the number of cells in the SEM image are calculated by Image J.

The cell size was obtained by measuring the maximum diameter of each cell perpendicular to the skin.

The cell density (N_0) is given by the following equation.

$$N_0 = \left(\frac{nM^2}{A}\right)^{3/2} \times \Phi \quad (4)$$

Where n is the number of cells in the SEM image, M is the magnification of the picture, and Φ is the volume expansion ratio, A is the area of the SEM image.

3. Results and discussion

3.1 Gel content of the NA-PAEK films

The crosslinking mechanism of NA-PAEK is displayed in **Scheme S11**, and the gel contents of the NA-PAEK films crosslinked at various temperatures are listed in **Table 1**. As evident from **Table 1**, after crosslinking the gel content of the NA-PAEK films increased with an increase in the crosslinking temperature. These films will be referred to hereafter as Gel 0%, Gel 18%, Gel 48%, and Gel 95%, according to the measured gel content values.

Table 1 Gel contents of NA-PAEK films crosslinked at different temperature

Crosslinking Temperature (°C)	Untreated	170	200	250
Gel Content (wt. %)	0	18	48	95

3.2 Dynamic mechanical analysis

Fig.1 displays the storage modulus and loss tangent ($\text{Tan}\delta$) of NA-PAEK films with different gel content. From **Fig.1**, it can be found that the storage modulus of NA-PAEK films gradually increases with the increase in the gel content or the degree of crosslinking. This means that the elasticity of NA-PAEK films gradually enhances with increasing the degree of crosslinking. In addition, the peak value of $\text{Tan}\delta$ also increases with the increase in the gel content or the degree of crosslinking. This further proves the effective formation of the crosslinking network to limit the segment motion of NA-PAEK.

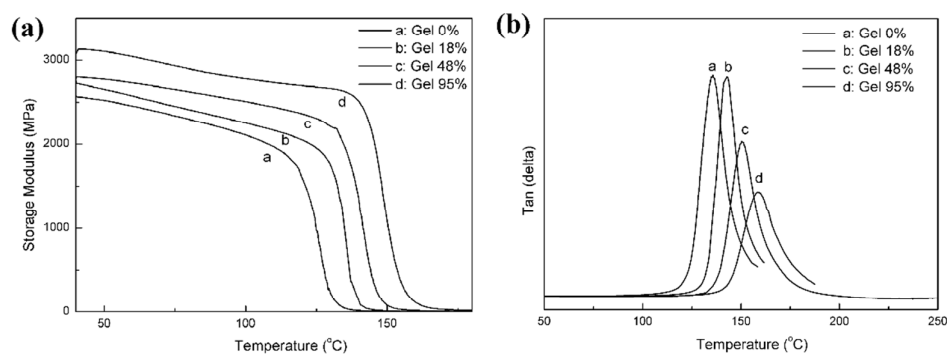


Fig.1 Storage modulus (a) and $\text{Tan}\delta$ (b) of NA-PAEK films with different gel content.

3.3 Thermal stability

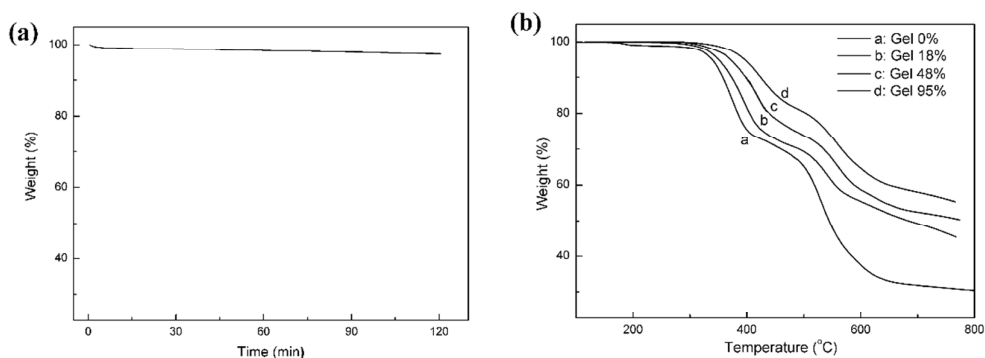


Fig.2 (a). TGA curve of sample with gel content 0% heated in air for 2 h at 250°C. (b) TGA curves for samples with different gel content heated in N_2 from 100°C to 800°C.

TGA data of o NA-PAEK films with different gel content are displayed in **Fig.2**. First NA-PAEK film with gel content 0% was heated in air for 2 h at 250 °C to make sure if there was degradation during the crosslinking process. From **Fig.2a**, it can be seen that the weight loss of the above treated film is very small, which proves that almost no degradation occurred during the crosslinking process. Then samples with different gel content were heated in N_2

from 100°C to 800°C to measure the thermal stability of the crosslinked samples. Obviously, the thermal stability of samples increased with increasing the gel content in **Fig.2b**.

3.4 Absorption and desorption of CO₂

The amount of CO₂ absorbed by the sample is a critical factor that determines the foam morphology during the supercritical foaming process. In fact, high CO₂ absorption is expected to increase the number of nucleation sites in the sample, and consequently, the cell density, which is an important characteristic of the nanocellular foam, will increase. Therefore, a detailed investigation was conducted to understand the influence of gel content, soaking pressure, and soaking time on the CO₂ uptake.

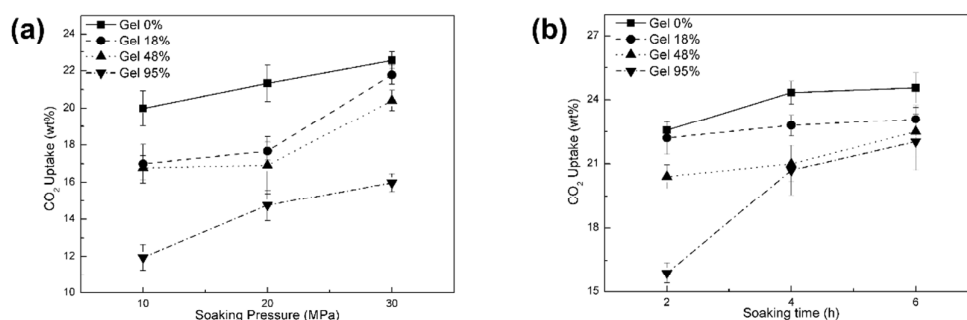


Fig. 3 (a) The relationship between soaking pressure and CO₂ uptake for NA-PAEK films with different gel contents and; (b) the relationship between soaking time and CO₂ uptake for NA-PAEK films with different gel contents

Experiments were carried out to determine the relationship CO₂ uptake in the NA-PAEK films with different gel content with soaking pressure. The films were saturated with CO₂ in the high pressure vessel for 2 h at room temperature, and the pressure chosen was 10, 20, and 30 MPa. The CO₂ uptake as a function of the soaking pressure is shown in **Fig. 3a**. As evident from the figure, the weight percentage of CO₂ uptake increases with the increase of soaking pressure for all the samples. That means high saturating pressure is in favor for absorbing more CO₂.¹⁶

The effect of soaking time on the CO₂ uptake was investigated next and the results are shown in **Fig. 3b** and **Fig. 4**. The pressure was set at 30 MPa and soaking times of 2, 4, and 6 h were studied in **Fig. 3b**. The NA-PAEK films with gel contents of 0, 18, and 48% exhibited only a slightly increase in the CO₂ uptake with increase in soaking time, while the sample with a gel content of 95% presented a sudden increase in CO₂ uptake when soaking time was increased from 2 to 4 h. This phenomenon can be attributed to the occurrence of crosslinking increased the tortuosity of the pathway when CO₂ entering the polymer, thus resulting in a longer time for the polymer/gas

system to reach equilibrium. It should be noted that the amount of CO₂ absorbed at zero time was determined by the intercept of straight line in Fig. 4.

Additionally, we can find from Fig. 3 that the CO₂ uptake by the NA-PAEK films decreased as the gel content increased, which should be ascribed that the occurrence of crosslinking reduces the free volume of NA-PAEK, and restricts the movement of polymer segments, which are both adverse to the dissolving of CO₂.

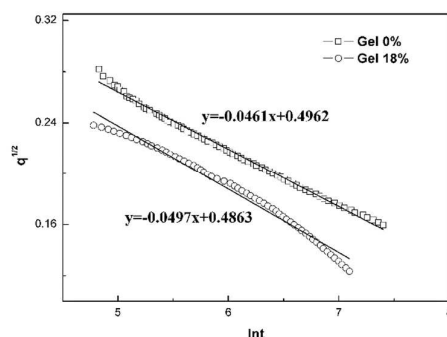


Fig.4 The square root of CO₂ concentration as a function of the logarithm of time for NA-PAEK films with Gel 0 % and Gel 18 %

3.5 Influence of gel content and foaming conditions on foam morphology

Besides optimizing the characteristics of the polymers, processing parameters at each stage of the discontinuous foaming method also need be optimized for the successful fabrication of nanocellular polymeric foams. Various factors such as soaking pressure, soaking time, transferring time, foaming temperature, and foaming time affect the foam morphology and the effects of these parameters on the foam morphology were studied.

3.5.1 Gel content and soaking pressure

The influence of gel content and soaking pressure on the foam morphology was first investigated. NA-PAEK films with different gel contents were saturated with CO₂ in a high-pressure vessel for 2 h at pressures of 10, 20, and 30 MPa. The films were then foamed in a glycerol bath at 140 °C for 60 s. The transferring time was set at 40 s. As shown previously, high soaking pressures are conducive for the absorption of CO₂. As evident from Fig. 5 and Fig. 6a, an increase in the soaking pressure from 10 to 30 MPa induced a considerable decrease in the cell size for all the NA-PAEK foam samples. In the case of the Gel 0% sample, the average pore size decreased from 4.13 to 2.5 μm when the soaking pressure was increased from 10 to 20 MPa. However, further increase in the soaking pressure to 30 MPa resulted in cell coalescence and the absence of a foamed structure. This was attributed to the high CO₂ uptake, which strongly plasticised the polymer and greatly lowered its elasticity, rendering the polymer incapable of supporting cell formation. For the Gel 18%, Gel 48%, and Gel 95% films, the cell sizes decreased continuously

with increase in the soaking pressure.¹⁷ It may be noted that the cell size for the Gel 18% sample decreased from 2.08 μm at 10 MPa to 320 nm at 30 MPa, thereby transforming from microcellular to nanocellular foam as the soaking pressure was increased from 10 to 30 MPa. On the other hand, the opposite trend was observed in the cases of cell density and volume expansion ratio (Fig. 6b and Fig. 6c), which increased continuously as the soaking pressure was increased from 10 to 30 MPa, for all the NA-PAEK foam samples. It is worth noting that among the NA-PAEK samples with various gel contents, the cell density of the Gel 18% increased most significantly, from 7.08×10^{10} at a soaking pressure of 10 MPa to 1.29×10^{12} at a soaking pressure of 30 MPa.

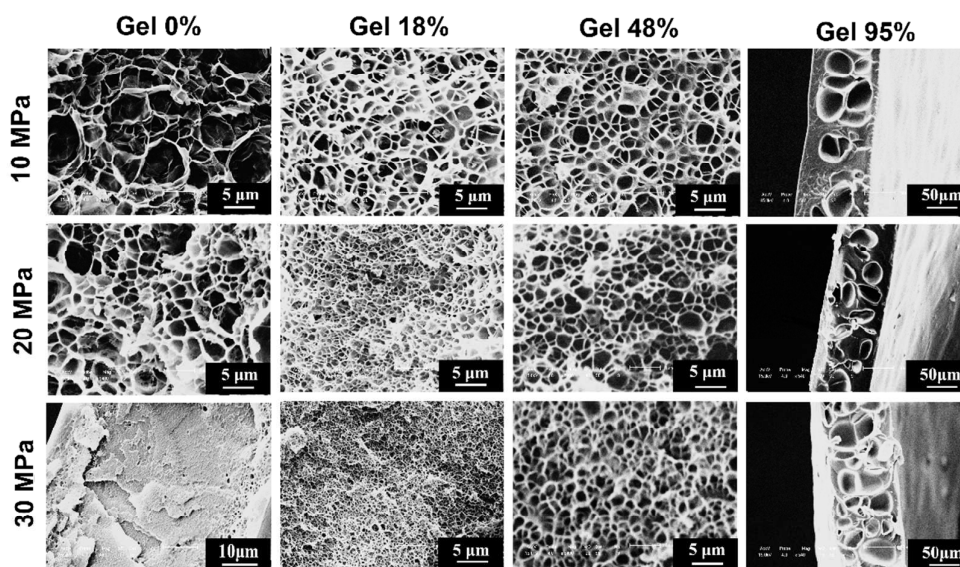


Fig. 5 SEM images of NA-PAEK foam samples with different gel contents prepared at soaking pressures of 10, 20, and 30 MPa (soaking time: 2 h, transferring time: 40 s, foaming temperature: 140 °C, and foaming time: 60 s).

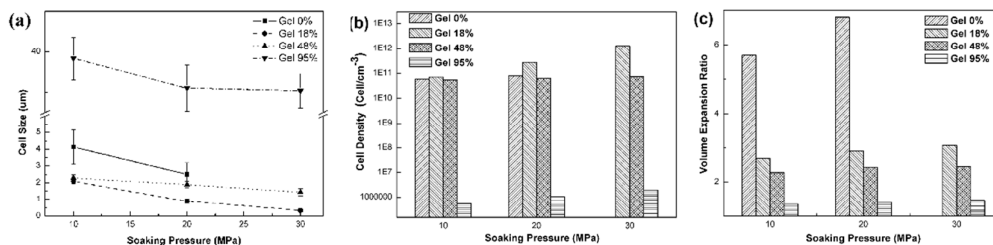


Fig. 6 The effect of soaking pressure on (a) cell size, (b) cell density, and (c) volume expansion ratio for NA-PAEK foams with different gel contents (soaking time: 2 h, transferring time: 40 s, foaming temperature: 140 °C, and foaming time: 60 s).

The elasticity of the polymer is expected to increase with increase in the gel content of NA-PAEK and the enhancement in elasticity is likely to limit the cell growth. As seen in **Fig. 5** and **Fig. 6c**, the volume expansion ratio decreased with increasing gel content at all soaking pressure values. At a soaking pressure of 10 MPa, the volume expansion ratio decreased from 5.69 for the Gel 0% sample to 1.34 for the Gel 95% sample. A similar tendency was seen at soaking pressures of 20 and 30 MPa.

In contrast, the cell density initially increased with increase in the gel content from 0 to 18%, beyond which it decreased steadily between gel contents of 18% and 95%, at all soaking pressure values (**Fig. 6b**). The change in the cell size with gel content was in the opposite direction as the change in the cell density with gel content (**Fig. 6a**). In other words, the cell size first decreased as the gel content was increased from 0 to 18%, following which the cell size continuously increased from gel contents of 18% to 95%. When the gel content was increased from 0% to 18%, the increase in the cell density was mainly due to the suppression of cell coalescence as a result of the increase in the elasticity of the polymer¹⁸. The change in the cell density and cell size with increase in the gel content from 18 to 95% can be explained by the nucleation theory.

As described by Youn *et al.*,¹⁹ the free energy required for the polymer/gas system to form nucleated bubbles is given by Eq. 5:

$$F = \sum_i u_i N_i + \sum_j A_j \gamma_j - PV + SE \quad (5)$$

where u_i is the chemical potential of component i , N_i is the mole number, γ_j is the interfacial energy of component j , A_j is the interfacial area, P is the pressure, V is the volume, and SE is the stored elastic energy in the system.

Since the volume of the bubble nucleus is very small, the change in the chemical potential can be neglected. In the system considered by Youn, SE was also negligible, since the matrix was in the liquid state when nucleation occurred. However, SE cannot be neglected in our experiments, since the matrix polymer is in a temporary high-elastic state and the elasticity of the matrix polymer increased with an increase in the crosslinking degree. Therefore, in our case, the minimum work required for homogeneous nucleation may be expressed by Eq. 6:

$$\Delta F = F_1 - F_2 = 4\pi r^2 \gamma - \frac{4\pi r^3}{3} \Delta P + \Delta SE \quad (6)$$

where r is the cell radius, Δp is the pressure difference between the supersaturation pressure and the environmental pressure, and ΔSE represents the change in the elastic energy stored in the system.

If E is the value of the stress per unit area caused by the elasticity of polymer when nucleating took place, then ΔSE can be given by the following equation:

$$\Delta SE = \frac{4\pi r^3}{3} E \quad (7)$$

Then the minimum work required for homogeneous nucleation (ΔF) becomes:

$$\Delta F = 4\pi r^2 \gamma - \frac{4\pi r^3}{3} \Delta P + \frac{4\pi r^3}{3} E \quad (8)$$

The critical radius (r_c) is reached when the free energy change with respect to the bubble size becomes zero.

$$\frac{d\Delta F}{dr} = 0 \quad (9)$$

At this point, the free energy reaches a maximum, and nuclei with radius larger than r_c remain stable and continue to grow. From this equation we can get that:

$$r_c = \frac{2\gamma}{\Delta P - E} \quad (10)$$

Therefore, in our experiments, the energy barrier required for nucleation may be given by Eq. 11:

$$\Delta G_c = \frac{16\pi\gamma^3}{3(\Delta P - E)^2} \quad (11)$$

In addition, the rate of homogeneous nucleation may be given by Eq. 12:

$$N_{hom} = C_0 f_0 e^{-\Delta G_c / KT} = C_0 f_0 e^{-\frac{16\pi\gamma^3}{3(\Delta P - E)^2 KT}} \quad (12)$$

Where C_0 is the gas concentration and f_0 is the frequency factor of the gas molecules.

The CO₂ uptake was shown to decrease with increasing gel content in the NA-PAEK films. Consequently, the gas concentration (C_0) in the supersaturated polymer/gas system will correspondingly decrease and ΔSE will simultaneously increase with increasing gel content in the NA-PAEK films. According to Eq. 12, the rate of nucleation will decrease with increasing gel content in the NA-PAEK films. With a lower rate of nucleation, the gas in the supersaturated system will continue to diffuse into the few available nucleated cells, allowing the cells to grow larger. This explains the decrease in the cell density and the increase in the cell size of the NA-PAEK foam with an increase in the gel content from 18 to 95%, observed in our previous experiments.

3.5.2 Foaming temperature

To investigate the influence of foaming temperature on the foam morphology, NA-PAEK film with a gel content of 18% was foamed in a glycerol bath in the temperature range of 100-160 °C. The soaking pressure, soaking time, transferring time, and foaming time were set at 30 MPa, 2 h, 40s, and 60 s, respectively.

As evident from **Fig. 7** and **Fig. 8a**, the volume expansion ratio initially increased with an increase in the temperature from 100 to 140 °C, following which it decreased with an increase in the temperature from 140 to 160 °C.²⁰ As shown in **Fig. 8b**, the cell density also increased with an increase in the foaming temperature from 100 to 120 °C, beyond which it decreased as the temperature was increased from 120 to 160 °C. In contrast, the cell size first decreased with an increase in the temperature to 120 °C, following which it increased as the temperature was increased from 140 to 160 °C, as shown in **Fig. 8c**. This can be explained by considering the influence of

temperature on the elasticity of the matrix polymer. Since the elasticity is expected to decrease with an increase in the foaming temperature, the nucleation rate is likely to increase with an increase in the temperature, as evident from Eq. 12. With an increase in the nucleation rate, cell density and volume expansion ratio will increase, whereas the cell size will decrease. However, as the temperature continues to increase, the decreased elasticity will become incapable of supporting all the cells. Therefore, cell coalescence will occur, leading to an increase in the cell size. On the other hand, the volume expansion ratio and cell density will decrease with further increase in the temperature.

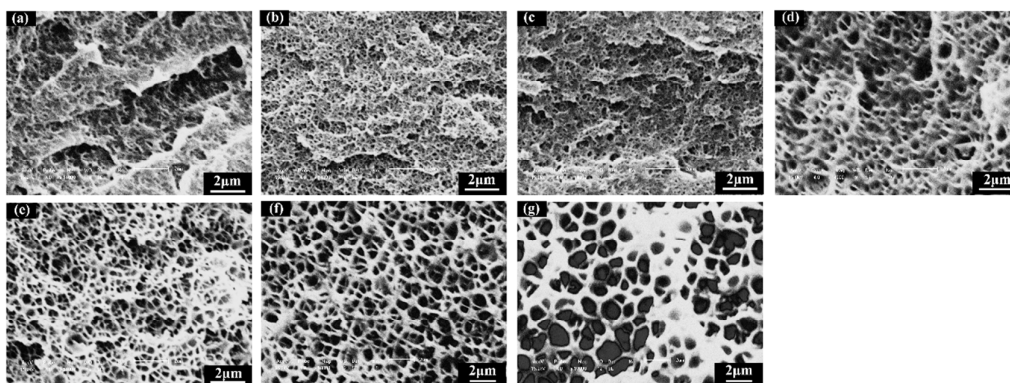


Fig. 7 SEM images of NA-PAEK foams with gel content 18% prepared at foaming temperatures of

(a) 100 °C, (b) 110 °C, (c) 120 °C, (d) 130 °C, (e) 140 °C, (f) 150 °C, and (g) 160 °C.

(soaking pressure: 30 MPa, soaking time: 2 h, transferring time: 40 s, and foaming time: 60 s).

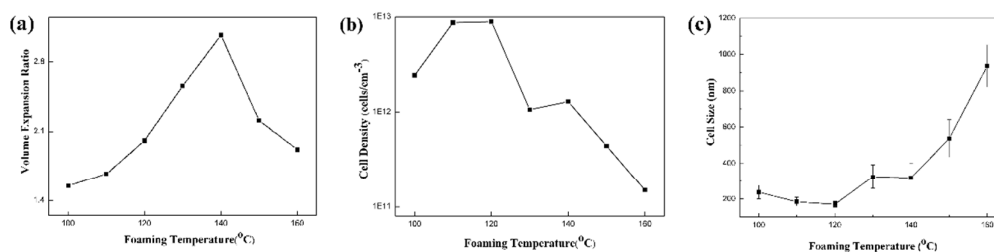


Fig. 8 The effect of foaming temperature on (a) volume expansion ratio, (b) cell density, and (c) cell size for NA-PAEK foam with a gel content of 18% (soaking pressure: 30 MPa, soaking time: 2 h, transferring time: 40 s, and foaming time: 60 s)

3.5.3 Soaking time

It is already known that longer soaking time is beneficial for CO₂ absorption. To investigate the effect of soaking time on the foam morphology of NA-PAEK films, NA-PAEK film with a gel content of 18% was saturated with CO₂ in the high-pressure vessel at a soaking pressure of 30 MPa for 2, 4, and 6 h. The sample was then foamed in

a glycerol bath. The transferring time, foaming temperature, and foaming time were 40 s, 120 °C, and 60 s, respectively.

From **Fig. 9** and **Table 2**, it can be seen that the volume expansion ratio and cell density increased with an increase in the soaking time. However, the cell size decreased with an increase in the soaking time. When the soaking time was 6 h, nanocellular foam with a cell size of 86 nm (± 11 nm) was produced.

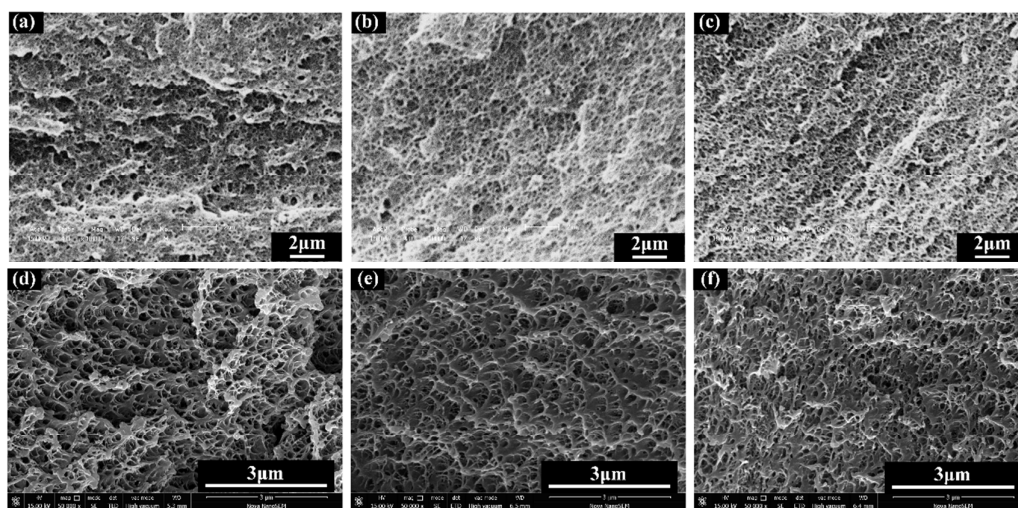


Fig. 9 SEM images of NA-PAEK foams with a gel content of 18% prepared with soaking times of (a) (d) 2 h, (b) (e) 4 h, and (c) (f) 6 h (soaking pressure: 30 MPa, transferring time: 40 s, foaming temperature: 120 °C, and foaming time: 60 s)

Table 2 Volume expansion ratio, cell size, and cell density of NA-PAEK foams with a gel content of 18% prepared with different soaking times at a soaking pressure of 30 MPa, transferring time of 40 s, foaming temperature of 120 °C, and foaming time of 60 s

Soaking time	2h	4h	6h
Volume expansion ratio	2.01	2.12	2.22
Cell density (cells/cm ³)	8.91×10^{12}	1.14×10^{13}	1.5×10^{13}
Cell size (nm)	172	166	86
Standard deviation	16	23	11

3.5.4 Transferring Time

The escape of gases during the transfer process is unavoidable. Therefore, it is important to understand the effect of transferring time on the foam morphology. For this purpose, Gel 18% NA-PAEK films with transferring times

of 40 s, 2 min, and 5 min were foamed in a glycerol bath and the samples were examined using SEM (Fig. 10). The soaking pressure, soaking time, foaming temperature, and foaming time were set at 30 MPa, 6 h, 120 °C, and 60 s, respectively. Fig. 10 shows that the cell size increased with an increase in the transferring time because of the gas escaping from the film.¹⁶

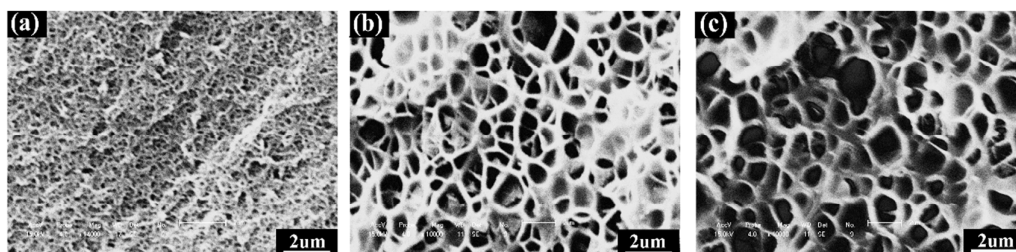


Fig. 10 SEM images of Na-PAEK foams with a gel content of 18% prepared with transferring times of (a) 40 s, (b) 2 min, and (c) 5 min (soaking pressure: 30 MPa, soaking time: 6 h, foaming temperature: 120 °C, and foaming time: 60 s)

3.5.5 Foaming time

To investigate the influence of foaming time on the foam morphology, Gel 18% Na-PAEK film was foamed in the glycerol bath for 10 s, 30 s, 1 min, 2 min, and 5 min and the samples were examined using SEM (Fig. 11). The soaking pressure, soaking time, transferring time, and foaming temperature were set at 30 MPa, 6 h, 40 s, and 120 °C, respectively. It can be seen from Fig. 11 that the foam morphology did not change much as a function of foaming time, implying that the foaming process was complete within 10s, as a result of which longer foaming times had little influence on the foam morphology.

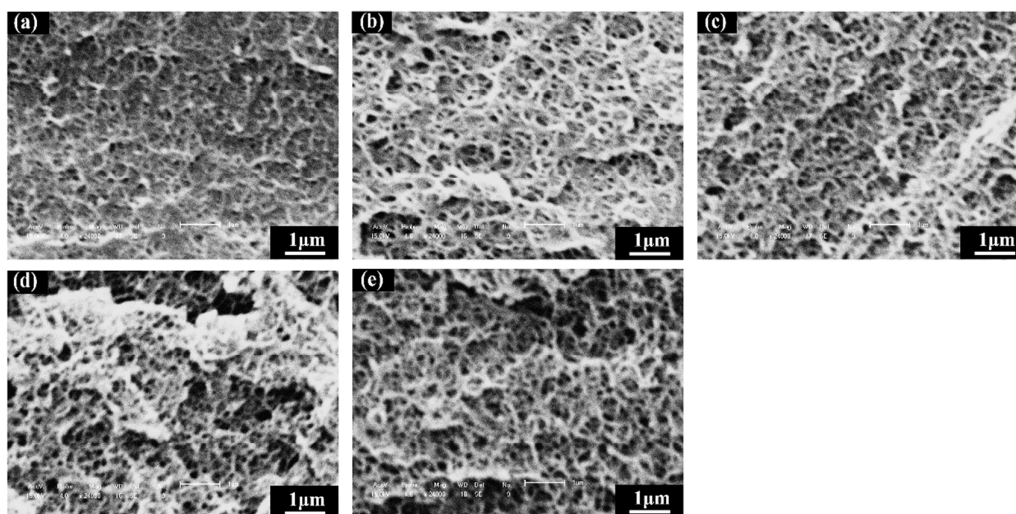


Fig. 11 SEM images of NA-PAEK foams with a gel content of 18% prepared with foaming times of (a) 10 s, (b) 30

s, (c) 60 s, (d) 2 min, and (e) 5 min (soaking pressure: 30 MPa, soaking time: 6 h, transferring time: 40 s, and foaming temperature: 120 °C)

4. Conclusion

NA-PAEK films with different crosslinking degrees were foamed using a two-stage batch foaming process. The crosslinking degree of the film was found to significantly influence the absorption of CO₂ and the foam morphology. It was first discovered that for a highly elastic polymer matrix, the stored elastic energy in the system (SE) during nucleation cannot be neglected, and it is a key factor influencing the nucleation rate and foam morphology. Experiments showed that the slight increase of crosslinking degree decreased the cell size and amplified the cell density because it successfully suppressed the cell coalescence. However, further increase of crosslinking degree increased the cell size and lowered the cell density because of the reduction of nucleation rate. By controlling the crosslinking degree and optimizing the processing parameters, nanocellular foam with a cell size of 86 nm (± 11 nm) was successfully fabricated, which is suitable for application as low-k and thermal insulation materials under high temperatures.

Acknowledgment

This work was financially supported by the National Nature Science Foundation of China (51203060) as well as Jilin province science and technology development program of China (20140203005GX).

References

1. A. Zhang, Q. Zhang, H. Bai, L. Li, and J. Li, *Chem. Soc. Rev.*, 2014, **43**, 6938-6956.
2. C. Forest, P. Chaumont, P. Cassagnau, B. Swoboda, and P. Sonntag, *Prog. Polym. Sci.*, 2014, **79**, 6700-6724.
3. S. Costeux, *J. Appl. Polym. Sci.*, 2014, **131**, 41293-41309.
4. B. Notario, J. Pinto, E. Solorzano, J. a. de Saja, M. Dumon, and M. A. Rodríguez-Pérez, *Polymer*, 2014, **32**, 3861-3872.
5. I. Cooper, *Adv. Mater.*, 2003, **15**, 1049-1059.
6. D. Miller and V. Kumar, *Polymer*, 2009, **50**, 5576-5584.
7. D. Miller and V. Kumar, *Polymer*, 2011, **52**, 2910-2919.
8. S. Costeux and L. Zhu, *Polymer*, 2013, **54**, 2785-2795.
9. H. Yokoyama and K. Sugiyama, *Macromolecules*, 2005, **38**, 10516-10522.
10. H. S. Wang, G. B. Wang, W. L. Li, Q. T. Wang, W. Wei, Z. H. Jiang and S. L. Zhang, *J. Mater. Chem.*, 2012, **22**,

21232-21237.

11. S. L. Zhang, H. S. Wang, Z. H. Jiang and G. B. Wang, *Appl. Phys. Lett.*, 2012, **101**, 012904-012904-4.
12. H. Wei, H. B. Zhang and Z. H. Jiang, *Chem. J. Chinese Univ.*, 2012, **33**, 33–36.
13. D. Wang, W. Jiang, H. Gao, Z. Jiang, *J. Memb. Sci.*, 2006, **281**, 203–210.
14. M. Pantoula and C. Panayiotou, *J. Supercrit. Fluid.*, 2006, **37(2)**, 254-262.
15. V. Kumar and J. Weller, *J. Eng. Ind.*, 1994, **116**, 413-420.
16. B. Krause, R. Mettinkhof, N. F. A. van der Vegt, and M. Wessling, *Macromolecules*, 2001, **34**, 874-884.
17. M. Tran, C. Detrembleur, M. Alexandre, C. Jerome, and J Thomassin, *Polymer*, 2013, **54**, 3261-3270
18. W. T. Zhai, H. Y. Wang, J. Yu, J. Y. Dong, J. S. He, *Polym. Eng. Sci.*, 2008, **48(7)**, 1312-1321.
19. Jae R. Youn and Nam P. Suh, *Polym. Compos*, 1985, **6**, 175–180.
20. D. Wang, W. Jiang, H. Gao, and Z. H. Jiang, *J. Polym. Sci. Polym. Phys.*, 2007, **45(2)**, 173-183.